AIP | Journal of Applied Physics

The induction of a graphite-like phase on diamond films by a Fe-coating/post-annealing process to improve their electron field emission properties

Pin-Chang Huang, Wen-Ching Shih, Huang-Chin Chen, and I-Nan Lin

Citation: Journal of Applied Physics **109**, 084309 (2011); doi: 10.1063/1.3569887
View online: http://dx.doi.org/10.1063/1.3569887
View Table of Contents: http://scitation.aip.org/content/aip/journal/jap/109/8?ver=pdfcov
Published by the AIP Publishing

The induction of a graphite-like phase on diamond films by a Fe-coating/post-annealing process to improve their electron field emission properties

Pin-Chang Huang,[1] Wen-Ching Shih,[1,a)] Huang-Chin Chen,[2] and I-Nan Lin[2]
[1]*Graduate Institute in Electro-Optical Engineering, Tatung University, Taipei 104, Taiwan*
[2]*Department of Physics, Tamkang University, Tamsui, New-Taipei 251, Taiwan*

(Received 15 December 2010; accepted 27 February 2011; published online 18 April 2011)

The electron field emission (EFE) process for diamond films was tremendously enhanced by Fe-coating and post-annealing processes. Microstructural analysis indicates that the mechanism for the improvement in the EFE process is the formation of nanographites with good crystallinity that surround the Fe (or Fe_3C) nanoclusters. Presumably the nanographites were formed via the reaction of Fe clusters with diamond films, viz. by the dissolution of carbons into Fe (or Fe_3C) clusters and the reprecipitation of carbon species to the surface of the clusters, a process similar to the growth of carbon nanotubes via Fe clusters as catalyst. Not only is a sufficiently high post-annealing temperature (900°C) required but also a highly active reducing atmosphere (NH_3) is needed to give a proper microstructure for enhancing the EFE process. The best EFE properties are obtained by post-annealing the Fe-coated diamond films at 900°C in an NH_3 environment for 5 min. The EFE behavior of the films can be turned on at $E_0 = 1.9$ V/μm, attaining a large EFE current density of 315 μA/cm^2 at an applied field of 8.8 V/μm (extrapolation using the Fowler–Nordheim model leads to $J_e = 40.7$ mA/cm^2 at a 20 V/μm applied field). © *2011 American Institute of Physics*. [doi:10.1063/1.3569887]

I. INTRODUCTION

Diamond films possess many desirable physical and chemical properties[1–3] and have been the focus of intensive research since the successful synthesis of diamonds in the low pressure and low temperature chemical vapor deposition (CVD) process.[4] Due to the negative electron affinity (NEA)[5] characteristics of the re-constructed (100) surface of diamond films, the diamond is considered to have great potential for applications as electron field emitters.[6,7] Generally, a good electron field emitter requires a sufficient supply of electrons from the back contact of materials, effective transport of electrons through the films, and efficient emission from the film surface. The large electronic bandgap (5.1 eV) of diamond films hinders their electron field emission (EFE) behavior tremendously due to the lack of conducting electrons required for field emission. Doping the diamond films with boron or nitrogen species provides abundant interband energy levels, which have been observed to markedly enhance both the supply of electrons and facilitate the transport of electrons and hence improve the EFE properties of the materials.[8–12] However, the EFE properties for these diamonds are still not satisfactory due to the fact that most of the emitting surfaces do not possess NEA characteristics because they are not re-constructed (100) surfaces. Modification of the surface characteristics of diamond to enhance the EFE process has thus been the main focus of research.[5,13–15] Among the various approaches, a thin metallic coating was observed to influence the EFE properties of diamond films prominently.[14] Post-treatment in an environment containing Fe species was also observed to tremendously improve the EFE properties of diamond,[15] but the related mechanism is not clear.

In this paper, the effect of Fe-coating and post-annealing processes on the surface characteristics and the EFE behavior of diamond films was systematically examined. Transmission electron microscopy (TEM) was used to investigate the microstructure of the films, and the possible mechanism is discussed based on the observations.

II. EXPERIMENTS

The diamond films were grown on a p-type silicon substrate by a microwave plasma enhanced CVD (MPE-CVD) process. The substrates were first thoroughly cleaned by the Radio Company of America (RCA) process,[16] which rinsed the Si wafer sequentially in water-diluted hydrogen peroxide/ammonium hydroxide and hydrogen peroxide/hydrochloric acid solution. The cleaned Si substrates were then ultrasonicated in a methanol solution containing nano-sized diamond powders and Ti powders (< 32.5 nm) for 45 min. The substrates were ultrasonicated again in methanol to remove the nanoparticles, which were possibly adhered on the Si substrates. The diamond films were grown in a $CH_4/H_2 = 1/99$ sccm plasma, excited by a 1400 W (2.45 GHz) microwave with a 55 Torr total pressure for 1 h. Thus the diamond films were designated as microcrystalline diamond (MCD) films. The MCD was then coated with a thin layer of Fe by a dc sputtering process for 1 min to a thickness around 5 nm and was designated as Fe/MCD film. They were then thermally post-annealed in an NH_3 (or H_2) atmosphere (100 sccm) for 5 min with heating and cooling rates of 15 °C/min. These films were designated as $(Fe/MCD)_{an}$ films.

a)Author to whom correspondence should be addressed. Electronic mail: wcshih@ttu.edu.tw.

The morphology and structure of the films were investigated with scanning electron microscopy (SEM, Joel JSM-6500F) and Raman spectroscopy (Renishaw inVia Raman microscopes), respectively. The detailed microstructure was examined using transmission electron microscopy (TEM, Joel 2100). The EFE properties of the diamond films were measured using a parallel plate setup in which the cathode-to-anode distance was set by a fixed spacer (125 μm) and the current-voltage (I-V) characteristics were acquired by a Keithley 2410 at 10^{-6} Torr. The EFE properties were analyzed by the Fowler–Nordheim (F-N) model,[17] and the turn-on field was designated as the interception of the lines extrapolated from the high- and low-field segments of the F-N plots.

III. RESULTS AND DISCUSSION

Figure 1(a) shows that post-annealing the Fe/MCD films in a reducing atmosphere (NH_3 or H_2) at 900 °C even for an interval as short as 5 min, tremendously improved the EFE behavior of the films. The turn-on field (E_0) decreased from 4.7 V/μm for the as-grown MCD films (curve I) to 2.8 V/μm (H_2) and 1.9 V/μm (NH_3) for post-treated films (curves III and IV). Notably, the NH_3 atmosphere imposed markedly better efficiency than the H_2 atmosphere in terms of enhancing the EFE for the films, that is, the EFE current density at an applied field of 8.8 V/μm is only $(J_e) = 39$ μA/cm^2 for the H_2-annealed Fe/MCD films (curve III) and is $(J_e) = 315$ μA/cm^2 for the NH_3-annealed Fe/MCD films (curve IV).

For the purpose of understanding how the Fe-coating and post-annealing processes improve the EFE properties of the MCD films and why the NH_3 atmosphere was much better than the H_2 atmosphere in terms of enhancing these characteristics, the modification of the EFE behavior of the MCD films due to these treatment processes was systematically investigated. Figure 1(b) shows the effect of the post-annealing temperature (800-950 °C, NH_3) on the EFE behavior of the Fe/MCD films. Although the low temperature NH_3 atmosphere post-annealing (800 and 850 °C) process insignificantly modified the EFE of the Fe-MCD films, that is, $(E_0)_{800-Fe/MCD} = 3.5$ V/μm and $(E_0)_{850-Fe/MCD} = 3.2$ V/μm [curves I and II, Fig. 1(b)], the 900 °C post-annealing temperature markedly enhanced the EFE of the films, that is, the turn-on field for inducing the EFE process of these films was lowered to $(E_0)_{900-Fe/MCD} = 1.9$ V/μm for the 900 °C-(Fe/MCD)$_{an}$ films [curve III, Fig. 1(b)]. The EFE capacity increased more than two orders of magnitude due to the increase in the post-annealing temperature from 850 to 900 °C, that is, the EFE current density at an 8.8 V/μm applied field increased from $(J_e)_{850-Fe/MCD} = 2.6$ μA/cm^2 for the 850 °C-(Fe/MCD)$_{an}$ films to $(J_e)_{900-Fe/MCD} = 315$ μA/cm^2 for the 900 °C-(Fe/MCD)$_{an}$ films. Further increases in post-annealing temperature to 925 and 950 °C markedly degraded the EFE properties. The turn-on field increased to $(E_0) = 2.4-2.9$ V/μm and the EFE current density (at 8.8 V/μm) decreased to $(J_e) = 60-65$ μA/cm^2 for 925 °C (or 950 °C) post-annealed Fe/MCD films [curves IV and V, Fig. 1(b)]. These EFE parameters are summarized in Table I.

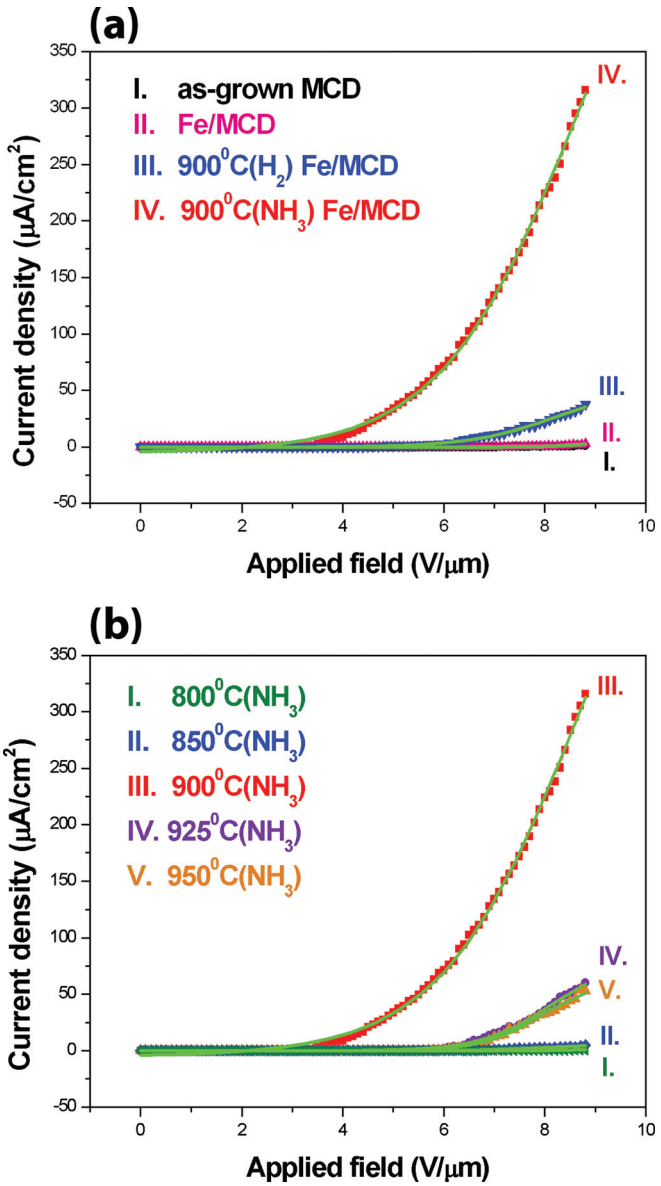

FIG. 1. (Color online) The electron field emission properties for the diamond (MCD) films (a) post-annealed at 900°C (5 min) in different reducing atmosphere; (iii) NH_3 and (iv) H_2 (where those for as-grown (i) and as Fe-coated (ii) MCD films were included to facilitate the comparison), (b) post-annealed in NH_3 atmosphere at different temperature; (i) 800°C, (ii) 850°C (iii) 900°C, (iv) 925°C, and (v) 950°C.

Post-annealing in H_2 atmosphere also modified the EFE properties for the (Fe/MCD)$_{an}$ films in a similar trend. Table I shows that the 900 °C post-annealing (in H_2) process also optimized the EFE properties for (Fe/MCD)$_{an}$ films as compared with those post-annealed in H_2 at other temperatures. The turn-on field (E_0) was larger and accompanied by a smaller EFE current density (J_e) for the films post-annealed either at lower (850 °C) or higher (950 °C) temperature. The EFE capacity (J_e) attainable at an applied field of 8.8 V/μm was only 39 μA/cm^2 for the Fe/MCD films post-annealed in H_2 (900 °C), which is eight times smaller than the J_e obtainable for the Fe/MCD films post-annealed in NH_3 (900 °C).

The Raman spectra shown in Fig. 2(a) indicate that the MCD films contain mainly the D-band resonance peak at 1332 cm^{-1} [curve I, Fig. 2(a)]. Small resonance peaks are

TABLE I. The EFE performance for Fe/MCD films annealed at different temperature and environment.

Samples	Annealing conditions: Atmosphere	Annealing conditions: Temperature (°C)	E_0[a] (V/μm)	J_e[b] (μA/cm^2)
MCD	-	-	4.7	0.84
Fe/MCD	-	-	3.67	0.55
(Fe/MCD)an	NH_3	800	3.5	<0.1
		850	3.2	2.6
		900	1.9	315.0
		925	2.4	65.0
		950	2.9	60.0
(Fe/MCD)an	H_2	850	3.4	14.5
		900	2.8	39.0
		950	3.4	26.0

[a]E_0: turn-on field designated as the interception of the lines extrapolated from the high field and low field segments in F-N plot.
[b]J_e: field emission current density measured at 8.8 V/μm.

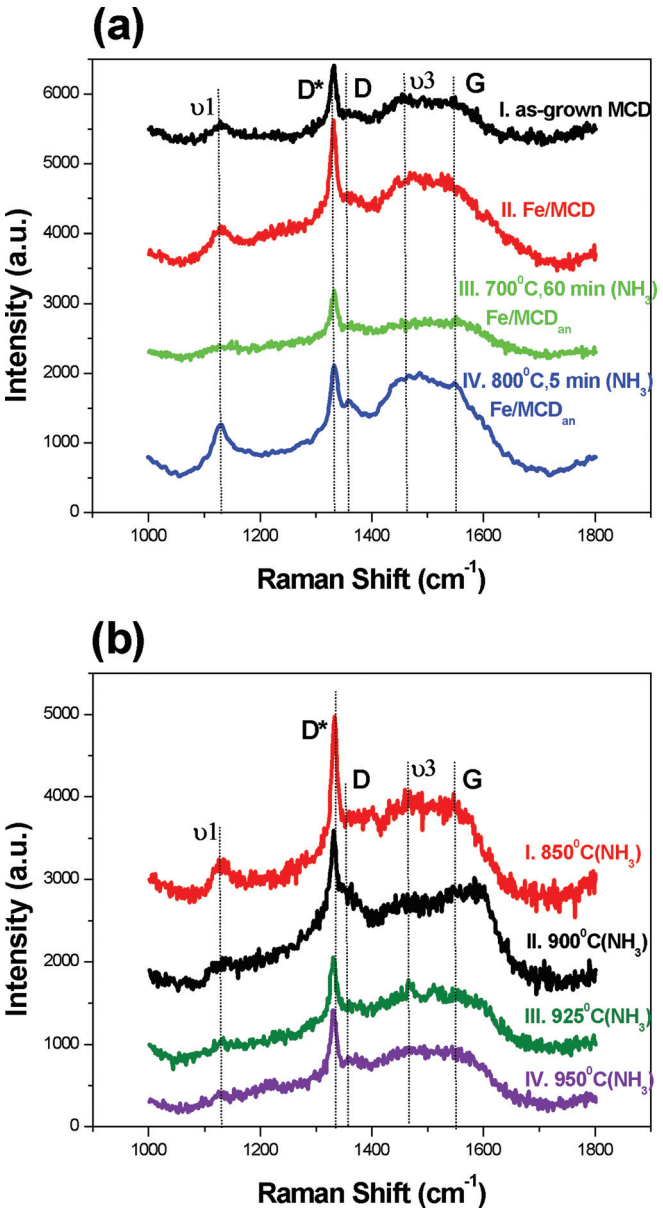

FIG. 2. (Color online) Raman spectroscopy for the diamond (MCD) films, which were (a) as-grown (i), coated with 10 nm of Fe (ii), Fe-coated and post-annealed at 700°C for 60 min in NH_3 atmosphere (iii), and Fe-coated and post-annealed at 800°C for 5 min in NH_3 atmosphere (iv); (b) those for MCD films, Fe-coated and post-annealed at (i) 800°C, (ii) 850°C (iii) 900°C, and (iv) 950°C for 5 min in NH_3 atmosphere.

also present near 1140 cm^{-1} (v_1-band) and 1480 cm^{-1} (v_3-band) and a broad resonance peak near 1580 cm^{-1} (G-band), indicating that the MCD films contain a small proportion of ultra-small diamond grains or residual graphitic phase. Visible Raman spectroscopy is several times more sensitive to the sp^2-bonded phase than to the sp^3-bonded one. The presence of sp^2-related Raman resonance peaks in these spectra does not imply that the MCD films contain a large proportion of sp^2-bonded materials. Fe-coating [curve II, Fig. 2(a)] and post-annealing at low temperature, 700 °C for 60 min [curve III, Fig. 2(a)] or 800 °C for 5 min [curve IV, Fig. 2(a)], hardly altered the Raman structure of the diamond materials. Figure 2(b) shows that the high-temperature post-annealing process also does not modify the Raman spectroscopy of Fe-MCD films except that the intensity of the D-band resonance peak and other resonance peaks decrease monotonically with the post-annealing temperature. The nondiamond resonance peaks (v_1-, v_3-, and G-bands) are almost completely nonobservable for the 925 °C (or 950 °C) post-annealed films [curves III and IV, Fig. 2(b)]. However, there is a broad resonance near 1600 cm^{-1} (G*-band), which is disorder graphite, for the 900 °C post-annealed films. The significance of such an extra resonance peak for the EFE behavior of this film will be discussed in the following text.

The enhancement in EFE properties is apparently resulted from the modification of the surface granular structure due to the post-annealing process. The SEM micrographs shown in Fig. 3(a) indicate that when the Fe-MCD films were post-annealed at 700 °C in an NH_3 atmosphere for 60 min, the thin Fe layer collapsed to form nanoclusters. The Fe clusters are still conducting, which is implied by the black contrast in the SEM images for the clusters. The faceted granular structure for the MCD films is essentially unaltered. These results imply that the Fe-to-diamond interaction has not yet occurred. Figure 3(b) shows that the Fe-to-diamond interaction was initiated by the 800°C (5 min) post-annealing process. The occurrence of a rigorous interaction between the Fe and diamond is indicated by the phenomenon wherein the nanoclusters were converted from conducting to insulating. The insulating nature for the clusters is implied by the occurrence of the electrical charging phenomenon as the contrast of the nanodots in the SEM image changed from black to white in color. Moreover, the faceted granular structure was markedly distorted, but the contour of the "large-grain" microstructure can still barely be resolved. These results imply that the Fe-to-diamond interaction occurred athermally. The interaction can be triggered instantaneously once the post-annealing temperature reaches 800 °C, and it will not be induced at 700 °C no matter how long the post-annealing interval is. The EFE properties were hardly changed due to such a low temperature (<800 °C) post-annealing process (cf. Table I) because diamond is still the emission site.

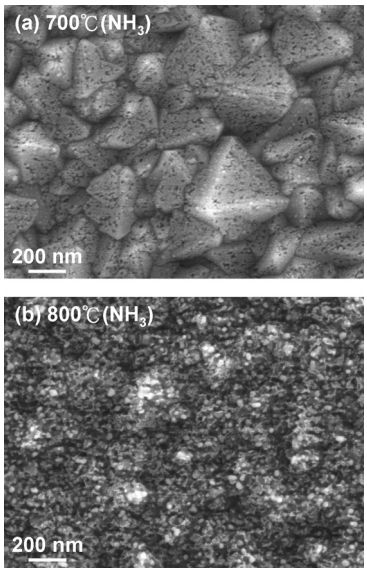

FIG. 3. SEM micrographs for diamond (MCD) films, which were Fe-coated and post-annealed at (a) 700°C for 60 min and (b) 800°C for 5 min in NH_3 atmosphere.

Figure 4 shows that post-annealing at a higher temperature (>850 °C) tremendously alters the surface morphology of the Fe-MCD films. When post-annealed at 850 °C (5 min), the clusters increased in size and the faceted granular structure was completely altered [Fig. 4(a)], but the clusters were still isolated from one another. When post-annealed at 900 °C (5 min), the clusters increased in proportion and almost formed a complete layer [Fig. 4(b)]. Further increases in post-annealing temperature to 950 °C (5 min) induced the agglomeration of the clusters, resulting in a networklike appearance [Fig. 4(c)]. Evidently, the SEM microstructure and Raman spectra were not able to elucidate the mechanism that leads to improved EFE properties for 900 °C-$(Fe/MCD)_{an}$ films. Detail microstructure analysis using TEM was necessary.

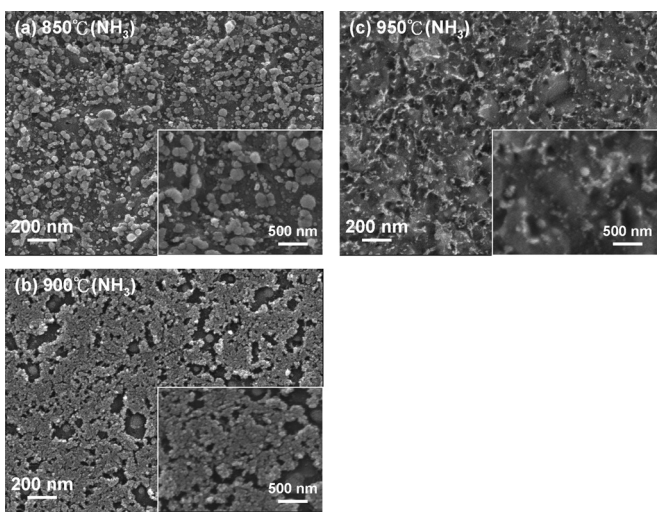

FIG. 4. SEM micrographs for diamond (MCD) films, which were Fe-coated and post-annealed at (a) 850°C (b) 900°C, and (c) 950°C for 5 min in NH_3 atmosphere.

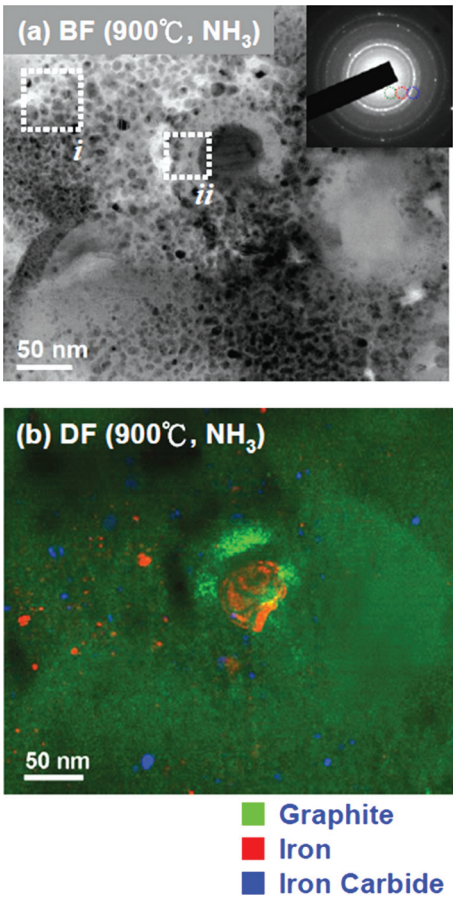

FIG. 5. (Color online) Low magnification (a) bright field and (b) dark field TEM micrographs for MCD diamond films, which were Fe-coated and post-annealed at 900°C for 5 min in NH_3 atmosphere.

Figure 5 shows a typical TEM micrograph of the 900 °C (NH_3) post-annealed Fe/MCD films. Numerous ultra-small clusters (~5–10 nm) are evenly distributed over the $(Fe/MCD)_{an}$ films. Selected area electron diffraction (SAED) in this figure indicates that the ultrasmall clusters are randomly oriented Fe_3C clusters. There are rare, residual large Fe particles distributed in the films. Dark-field images, which were taken from a different part of SAED [indicated as green, red, and blue circles in the inset of Fig. 5(a)], were superimposed to more clearly illustrate the distribution of the phase constituents. Figure 5(b) shows the distribution of the nanographite (green color), Fe particles (red color), and Fe_3C-clusters (blue color) contained in these films. The enlarged micrographs shown in Figs. 6(a) and 6(b) reveal, respectively, the detailed microstructures of the small cluster region [area "*i*", Fig. 5(a)] and the region near the large particles [area "*ii*", Fig. 5(a)] for the 900 °C(NH_3)-$(Fe/MCD)_{an}$ films. Fourier-transformed (FT) diffractograms of the corresponding area in Fig. 6(a) confirmed that the ultra-small clusters are Fe_3C particles about 5-10 nm in size [insets FT_1 and FT_2, Fig. 6(a)]. There are fringes about subnanometer in width that are a-few-layer graphite, surrounding the nano-Fe_3C clusters. The presence of nanographite surrounding the Fe_3C (or Fe) clusters is more clearly demonstrated in area 3 (FT_3) of Fig. 6(b), which is a region near the Fe large clusters [area "*ii*",

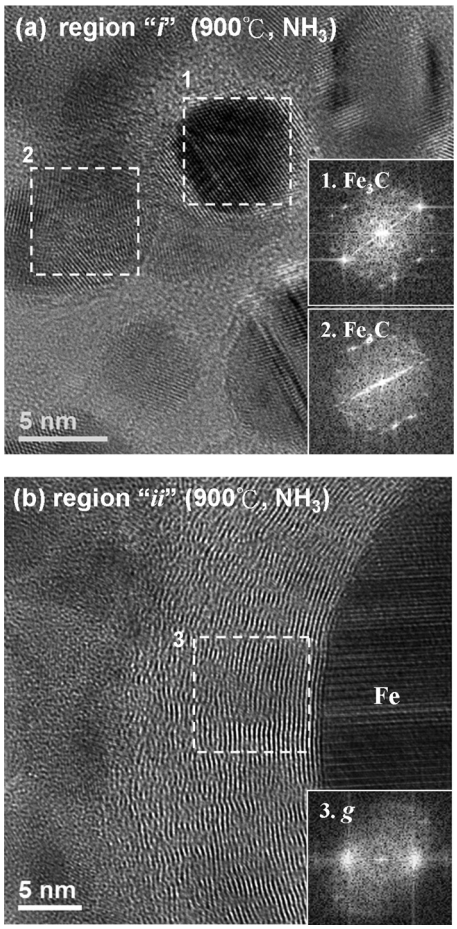

FIG. 6. TEM structure image for MCD diamond films, which were Fe-coated and post-annealed at 900°C for 5 min in NH_3 atmosphere, for the (a) "*i*" small cluster region and (b) "*ii*" large cluster region indicated in Fig. 5(a).

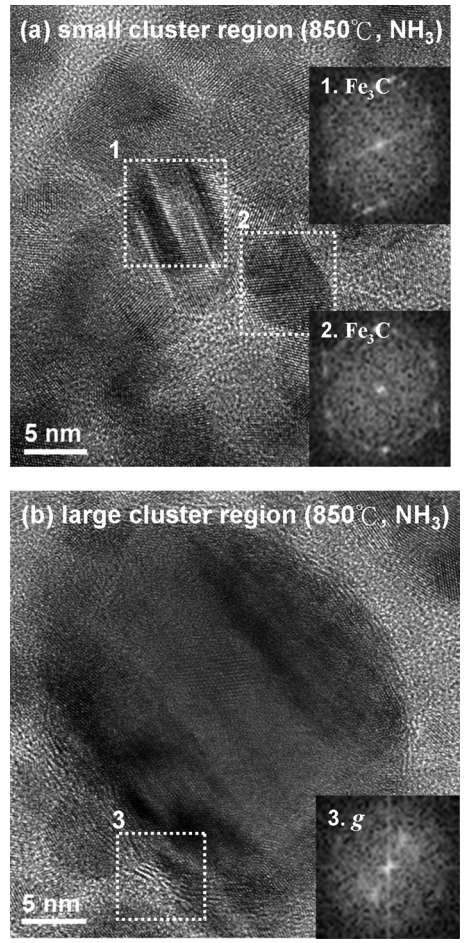

FIG. 7. TEM structure image for MCD diamond films, which were Fe-coated and post-annealed at 850°C for 5 min in NH_3 atmosphere, for the regions corresponding to (a) small cluster and (b) large Fe particles.

Fig. 5(a)]. The nanographite layers are about 12–15 nm in thickness.

Apparently, the presence of the nanographite not only enhances the transport of electrons but also facilitates the field emission process, a process similar to the EFE of the graphene composite.[18,19] The remaining unsolved question is how the nanographites are formed by the Fe-coating and post-annealing process. Before discussing the possible mechanism, it should be noted that the formation mechanism of carbon nanotubes (CNTs) has been proposed as follows. The carbon species are first dissolved into a catalyst and re-precipitated out, resulting in either a top- or bottom-growth process for CNTs.[20–23] Presumably, the same dissolution and re-precipitation processes also occur for the nano-sized Fe clusters formed on the diamond surface, which result in nano-sized graphites on the surface of these Fe clusters. The Fe_3C nanoclusters result when the Fe clusters, which contain some dissolved carbons, are cooled below the re-precipitation temperature.

A similar microstructure was observed for 850 °C(NH_3)-$(Fe/MCD)_{an}$ films except that the small clusters are lower in proportion (not shown). Figures 7(a) and 7(b) show the enlarged micrograph of the small and large cluster regions of these films, respectively. Again, the small clusters are Fe_3C (~5 nm) [areas 1~2, FT_1~FT_2, Fig. 7(a)], and the large clusters are Fe particles [~30 nm, Fig. 7(b)]. Notably, in 850 °C(NH_3)-$(Fe/MCD)_{an}$ films, there also exists a graphite layer surrounding the Fe particles [area 3 and FT_3, Fig. 7(b)], but the thickness of the graphite layer is thinner (~5 nm), and the crystallinity of the graphites is not as good compared with those in 900 °C(NH_3)-$(Fe/MCD)_{an}$ films. No clear graphite layer was observed to surround the small Fe_3C clusters. The lower abundance and inferior crystallinity in the nanographite phase for 850 °C(NH_3)-$(Fe/MCD)_{an}$ films are apparently the cause of the inferior EFE properties of these films compared with those of 900 °C(NH_3)-$(Fe/MCD)_{an}$ films. In other words, the 900 °C post-annealing process is required to induce abundant and crystalline nanographites to enhance the EFE process.

It is reasonable that a sufficient high post-annealing temperature is required to trigger the dissolution-reprecipitation process and to form nanographites with good crystallinity. Such a model accounts for the fact that the EFE properties of the 900 °C (NH_3)-annealed Fe-MCD films are superior to those of the 850 °C (NH_3)-annealed Fe-MCD films. However, the reason the post-annealing atmosphere in H_2 leads to such a different level of enhancement of the EFE properties of the films [cf. Fig. 1(a)] is still not clear. The low

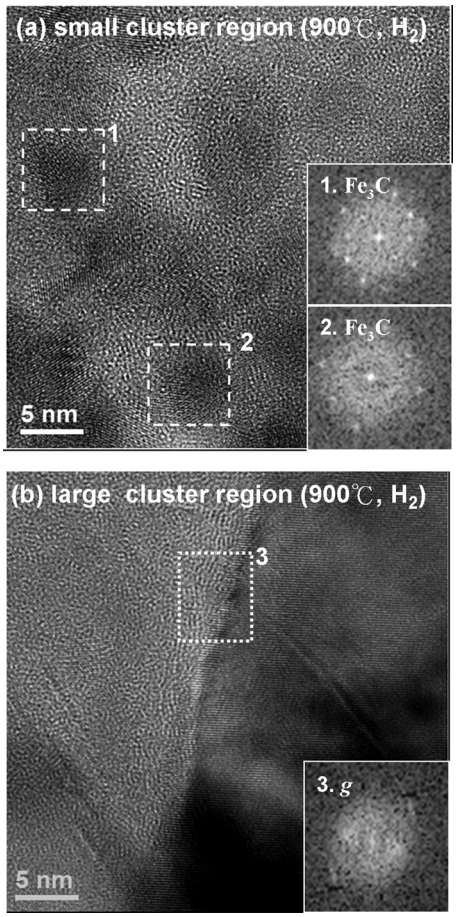

FIG. 8. TEM structure image for MCD diamond films, which were Fe-coated and post-annealed at 900°C for 5 min in H_2 atmosphere, for the regions corresponding to (a) small cluster and (b) large Fe particles.

magnification TEM investigation indicates that the 900 °C(H_2)-$(Fe/MCD)_{an}$ films also possess a microstructure similar to those for 900 °C(NH_3)-$(Fe/MCD)_{an}$ films (not shown). High magnification TEM micrographs for the 900 °C(H_2)-$(Fe/MCD)_{an}$ films shown in Fig. 8(a) indicate that the Fe_3C clusters are smaller (FT_1 and FT_2) with no surrounding graphite layer. Moreover, Fig. 8(b) shows that the graphitic layer near the Fe particles is thinner (3-4 nm) and inferior in crystallinity [area 3 and FT_3, Fig. 8(b)] compared with those of the 900 °C(NH_3)-$(Fe/MCD)_{an}$ films [cf. Fig. 6(b)].

It seems that both the dissolution/re-precipitation and crystallization processes were somehow hindered when the Fe-MCD films were post-annealed in an H_2 atmosphere. One possible explanation is that a native oxide may form instantaneously when the Fe-MCD films are transported from the sputtering chamber (Fe coating) to the annealing furnace. The native oxide cannot be efficiently removed when post-annealed in an H_2 environment but can be removed instantaneously when post-annealed in an NH_3 environment. Restated, the probable reason that the nanographites form more readily in the 900 °C(NH_3) post-annealing process is that when the Fe-MCD films were post-annealed in the H_2 atmosphere (at 900 °C), the residual oxidized layer slowed the re-precipitation and crystallization of carbon species in the formation of nanographite. In contrast, post-annealing in an NH_3 atmosphere readily reduced the oxidized Fe layer, which eliminated the deleterious effect of the native oxide layer on the re-precipitation and crystallization processes.

IV. CONCLUSIONS

The Fe-layer coated on micrometer-grain diamond, MCD, films was observed to coalescence to form small Fe clusters when post-annealed at 700 °C regardless of the post-annealing time. They started to react with diamond as soon as the post-annealing temperature reached 800 °C. Higher post-annealing temperature facilitated the carbon dissolution and re-precipitation processes, which markedly enhanced the EFE process for MCD films due to the Fe-coating and post-annealing processes. However, to achieve a proper microstructure and to enhance the EFE process, not only is a sufficiently high post-annealing temperature (900 °C) required but also a highly active reducing atmosphere (NH_3) is needed. Microstructural analysis indicates that the mechanism for the improvement of the EFE process is the formation of nanographites surrounding the Fe_3C (or Fe) nanoclusters, which were formed via the reaction of Fe clusters with diamond films. Presumably, the nanographites were formed by the re-precipitation of carbon species, which were dissolved in the Fe clusters in a process similar to the growth of carbon nanotubes via Fe clusters as catalyst. The best EFE properties achieved were a turn-on field of $E_0 = 1.9$ V/μm with an EFE current density of $J_e = 315$ μA/cm^2 at an applied field of 8.8 V/μm, which were obtained for the films post-annealed in the NH_3 environment at 900 °C for 5 min. The films post-annealed in the H_2 atmosphere exhibited inferior EFE behavior than those post-annealed in the NH_3 atmosphere, which is presumably due to the differences in the removal of the native oxide on Fe coatings.

ACKNOWLEDGMENTS

This work was sponsored by the Tatung University, and Tamkang University, Taiwan. The authors deeply appreciated their financial and technical support.

[1] J. E. Field, *The Properties of Diamonds* (Academic, London, 1979).
[2] H. Liu and D. S. Dandy, Diamond Relat. Mater. **4**, 1173 (1995).
[3] J. C. Angus, H. A. Will, and W. S. Stanko, J. Appl. Phys. **39**, 2915 (1968).
[4] B. V. Spitsyn, L. L. Bouilov, and B. V. Derjaguin, J. Cryst. Growth **52**, 219 (1981).
[5] J. van der Weide, Z. Zhang, P. K. Baumann, M. G. Wensell, J. Bernholc, and R. J. Nemanich, Phy. Rev. B **50**, 5803 (1994).
[6] M. W. Geis, N. N. Efremow, J. D. Woodhouse, M. D. Mcaleese, M. Marchywka, D. G. Socker, and J. F. Hochedez, IEEE Electron Device Lett. **12**, 456 (1991).
[7] W. P. Kang, J. L. Davidson, A. Wisitsora-at, D. V. Kerns, and S. Kerns, J. Vac. Sci. Technol. B **19**, 936 (2001).
[8] A. T. Sowers, B. L. Ward, S. L. English, and R. J. Nemanich, J. Appl. Phys. **86**, 3973 (1999).
[9] P. T. Joseph, N. H. Tai, H. Niu, U. A. Palnitkar, W. F. Pong, H. F. Cheng, and I. N. Lin, Diamond Relat. Mater. **17**, 1812 (2008).
[10] Y. C. Lee, S. J. Lin, I. N. Lin, and H. F. Cheng, J. Appl. Phys. **97**, 054310–1 (2005).
[11] C. F. Shih, K. S. Liu, and I. N. Lin, Diamond Relat. Mater. **9**, 1591 (2000).
[12] Y. H. Chen, C. T. Hu, and I. N. Lin, Appl. Phys. Lett. **75**, 2857 (1999).
[13] V. I. Polyakov, N. M. Rossukanyi, A. I. Rukovishnikov, S. M. Pimenov, A. V. Karabutov, and V. I. Konov, J. Appl. Phys. **84**, 2882 (1998).

[14]A. Lamouri, Y. Wang, G. T. Mearini, I. L. Krainsky, J. A. Dayton, Jr., and W. Mueller, J. Vac. Sci. Technol. B **14**, 2046 (1996).
[15]I. N. Lin, Y. H. Chen, and H. F. Cheng, Diamond Relat. Mater. **9**, 1574 (2000).
[16]W. Kern, J. Electrochem. Soc. **137**, 1887 (1990).
[17]R. H. Fowler and L. Nordheim, Proc. R. Soc. London Ser. A **119**, 173 (1928).
[18]G. Eda, H. E. Unalan, N. Rupesinghe, G. A. J. Amaratunga, and M. Chhowalla, Appl. Phys. Lett. **93**, 233502 (2008).
[19]Z. S. Wu, S. Pei, W. Ren, D. Tang, L. Gao, B. Liu, F. Li, C. Liu, and H. M. Cheng, Adv. Mater. **21**, 1756 (2009).
[20]D. C. Li, L. Dai, S. Huang, A. W. H. Mau, and Z. L. Wang, Chem. Phys. Lett. **316**, 349 (2000).
[21]E. F. Kukovitsky, S. G. L'vov, and N. A. Sainov, Chem. Phys. Lett. **317**, 65 (2000).
[22]S. B. Sinnott, R. Andrews, D. Qian, A. M. Rao, Z. Mao, E. C. Dickey, and F. Derbyshire, Chem. Phys. Lett. **315**, 25 (1999).
[23]A. Gorbunov, O. Jost, W. Pompe, and A. Graff, Carbon **40**, 113 (2002).